Wake interaction in high-KC oscillatory flow

Trygve Kristiansen, Henrik Reiten, Carlos Santamaria Izquierdo, Senthuran Ravinthrakumar and Bernard Molin

Department of Marine Technology, Norwegian University of Science and Technology (NTNU), Trondheim, Norway, *trygve.kristiansen@ntnu.no

The effect of hydrodynamic interaction between two or more bodies in *steady* flow has been examined in several papers in the literature, see for instance [1]. This has relevance in a large range of practical application, not only marine ones. The effect of *oscillatory* flow on *single* bodies has also been studied quite widely and was first understood by Keulegan and Carpenter. However, according to the authors' knowledge, none or very few studies have been conducted on the hydrodynamic interaction between *two or more cylindrical bodies in large-amplitude oscillatory flow*. This is the topic of the present paper. The results show that there are important wake interaction effects.

Our work was motivated by a type of floating solar island referred here to as a multi-modular structure, see Figure 1. The modules are connected by hinge-type connectors, and each module is supported by several slender pontoons. The pontoons may have different draft-to-side length ratio, cross-sectional shape and configured in different configurations. In typical configurations, the distance between nearby pontoons will be in the order of their cross-sectional dimension.

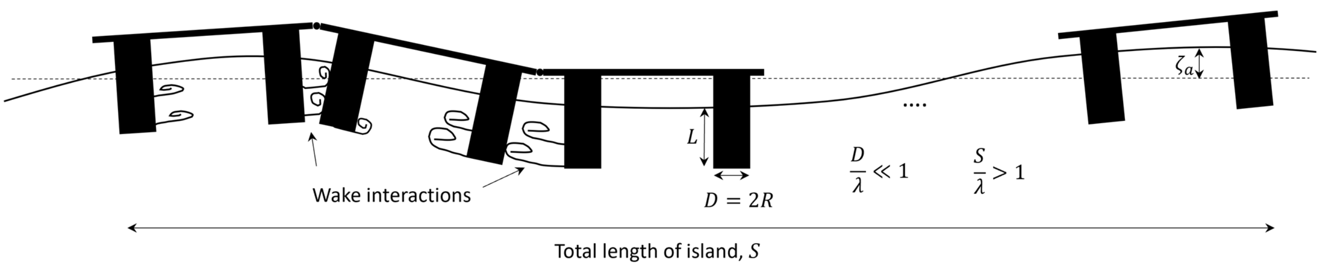

Figure 1. Sketch of a multi-modular structure, such as a floating solar island, in incident regular waves. Main parameters are wavelength λ, wave amplitude ζ_a, pontoon diameter D, total island length S. The pontoons will experience a near uniform horizontal oscillating flow $\lambda/D \gg 1$. We consider slender pontoons with $D \simeq 1\text{m}$.

The island follows the waves vertically to a large degree; this being the main principle for the multi-modular concept. On the other hand, due to the size of the whole island S relative to typical wavelengths λ, wave excitation cancellation effects imply negligible horizontal surge-type motions. The hydrodynamic loads will then to a large extent need to be absorbed by the connections. Further, typical wavelengths are much longer than the pontoon side-length, $\lambda/D \gg 1$, implying negligible potential flow type free-surface diffraction. Further, since also $\lambda/L \gg 1$, there is small variation in the vertical direction over the draft L of the pontoon. The pontoons will therefore experience a near uniform, horizontal, oscillatory flow, in which there will be hydrodynamic interactions due to the proximity of the pontoons. Wave amplitudes will be in the order of the pontoon side-length D, so the flow is characterized to be in the high KC-number range. For instance, if $D = 1.2\text{m}$ and $\zeta_a = 3\text{m}$, $\text{KC} = 2\pi\zeta_a/D \simeq 16$. Even higher KC-numbers may also be relevant.

The modules will in practice not follow the waves entirely in steep irregular waves, and there may be important effects due to time-varying wetted pontoon surface. There may also be wake-free-surface interactions. However, assuming these effects to be secondary, the free surface will to a first approximation act like an infinitely large splitter plate. We may then mirror the water above the free surface, meaning that we can consider cylinders with length $2L$ in infinite fluid. Given large length-to side-length ratio $2L/D \gg 1$, it is relevant to study the problem in a two-dimensional setting. Our present study is limited to physical experiments and CFD in a two-dimensional setting.

Wave flume experiments

In the experiments, cylinders in different configurations were forced to oscillate in sinusoidal motion in near infinite fluid conditions in a narrow wave flume at NTNU. The experimental set-up is illustrated in Figure 2. Several different configurations with two, four and eight cylinders were carried out. In the present work we present results from two configurations denoted Case 1 and Case 2. The cylinders had square cross-section with side-length $D = 0.03$m. The cylinder length was $L = 0.57$m. The Keulegan-Carpenter number is defined as $\mathrm{KC} = 2\pi\eta_{3a}/D$, where η_{3a} is the forced motion amplitude. KC-numbers from 0.5 to 24 were tested. Reynolds number scale effects are considered secondary due to sharp corners of the models with fixed flow separation points as a consequence, and sufficiently large Reynolds numbers for the wake to be turbulent. Empty rig tests (without model) were run and the measured forces from these tests were subtracted from the measured forces in the tests with model, time-step by time-step. In addition, the inertial force of each cylinder $M\ddot{\eta}_3$ was also subtracted; $M = 0.430$kg is the (dry) mass of each cylinder.

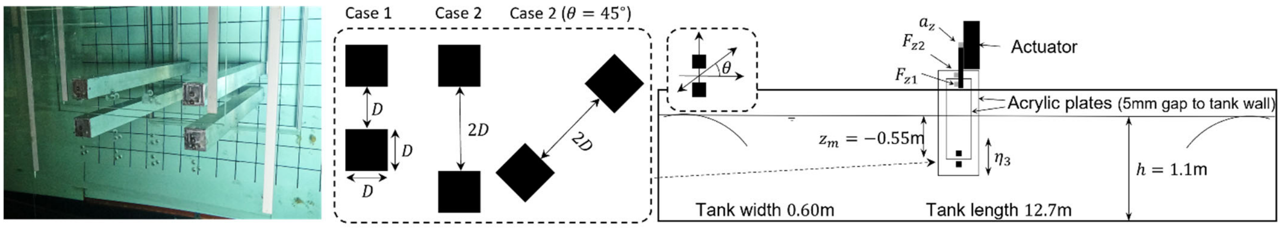

Figure 2. Experimental set-up. Forced oscillations achieved by a vertical actuator with vertical (inline) force measurement on each cylinder, denoted F_{z1} and F_{z2}. The models were connected to the force transducers via two separated acrylic plates on each side of the tank. The inflow angle θ is defined in the figure. Most tests were carried out for $\theta = 90°$. In Case 2, the cylinders were organized such as to also test $\theta = 45°$. $D = 0.030$m.

Results

Selected experimental force time-series from three relevant KC-numbers in Case 1 are presented in Figure 3. The forces are non-dimensionalized by the volume of the body and an acceleration based on the forcing period and cylinder side-length. The difference force $\Delta F = F_{z2} - F_{z1}$ is also included. The difference force is clearly increasing in magnitude with increasing KC-number. There is a pronounced 2ω-component emerging for the higher KC-numbers, in addition to a negative mean force component. The difference force ΔF matters for the connections, as it must partly be absorbed by these, and will receive a focus in this paper.

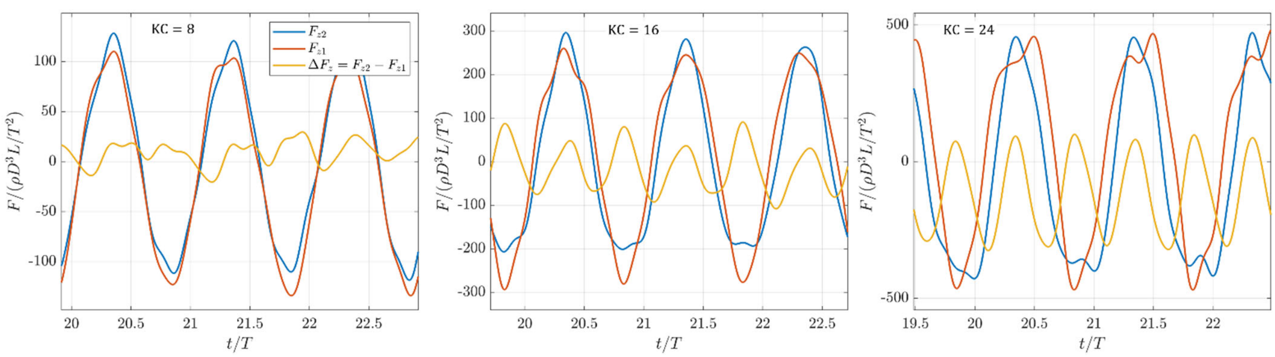

Figure 3. Experimental force time-series examples for three representatives KC-numbers from Case 1.

The amplitudes of the first three force harmonics for each of the two cylinders in Case 1 are presented as function of KC-number in the left part of Figure 4. The first harmonic force amplitude F_ω for a single two-dimensional square cylinder, as predicted by the Morison equation, is also included. The KC-dependent inertia and drag coefficients are obtained by curve-fitting to existing numerical and experimental data for a two-dimensional square cylinder in oscillatory flow with $\mathrm{KC} \leq 10$ (see for instance [3]), and assumed constant beyond this:

$$\begin{aligned} C_a(\mathrm{KC}) &= \alpha \mathrm{KC}^{2/3} + C_{a0} \ \text{ for } \ \mathrm{KC} \leq 10, \quad C_a = C_{a\infty} \ \text{ for } \ \mathrm{KC} > 10, \\ C_D(\mathrm{KC}) &= C_{D0} - \beta \mathrm{KC}^{2/3} \ \text{ for } \ \mathrm{KC} \leq 10, \quad C_D = C_{D\infty} \ \text{ for } \ \mathrm{KC} > 10. \end{aligned} \tag{1}$$

Here, $C_{a\infty} = 2.2$ deduced from visual inspection of the referred published data, $C_{D\infty} = 2.0$ as deduced from published data for steady flow, $\alpha = (C_{a\infty} - C_{a0})/10^{2/3}$ where $C_{a0} = 1.51$ is the zero-KC-number limit value according to potential flow theory, $\beta = (C_{D0} - C_{D\infty})/10^{2/3}$ where $C_{D0} = 4.0$ based on the published data. The measured first harmonic force amplitudes are quite similar as that predicted by the Morison model presented above for a single cylinder for $\mathrm{KC} \leq 15$. For larger KC-numbers the experimentally obtained force is smaller. The difference is believed to be due to hydrodynamic interaction between the two cylinders. We refer to this as *wake interaction* in this paper. The third harmonic force amplitude is also presented; that predicted by the Morison equation is significantly higher than that observed experimentally. We believe this is also a wake interaction effect, although we do not have other empirical data for the third harmonic force on a single square cylinder. Note that the force amplitudes are nearly equal for the two cylinders, indicating for instance minor free-surface effects.

The phase between the forces on the two cylinders are of importance; the first and third harmonic forces on each cylinder are in phase with each other, whereas the second harmonic forces are 180 degrees out of phase. This means that the difference force will be dominated by the second harmonic. Several harmonics of the difference force ΔF are presented in the right part of Figure 4. Clearly, the 2ω-component is dominant as compared to the other harmonics. Notable is that there is also a considerable mean difference force. The negative value means a suction force. This indicates that a cavity type flow is formed in-between the two cylinders, similar as in steady flow for cylinders with spacing below a critical value [1-2]. Perhaps more interestingly still is the large second harmonic force component.

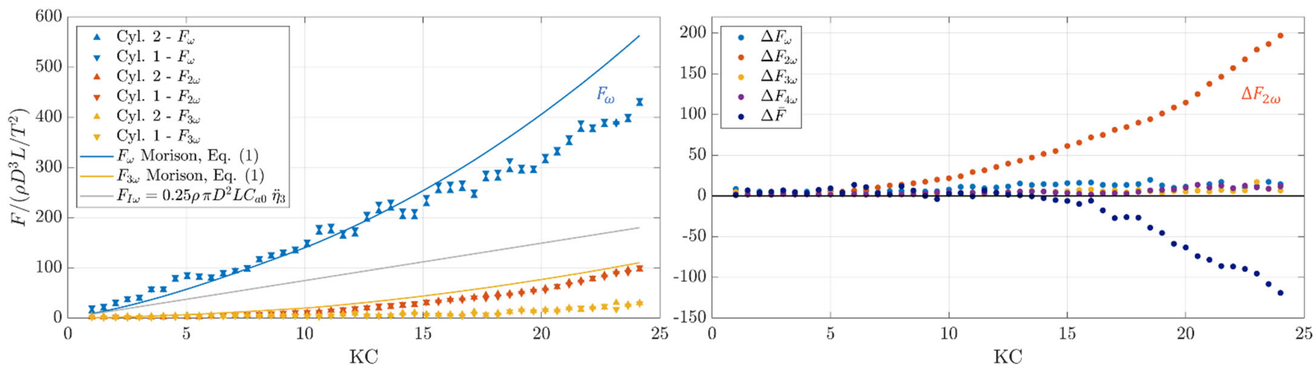

Figure 4. KC-number dependent force harmonic amplitudes for Case 1. Left: Force harmonic amplitudes for each cylinder. By Morison we refer to Morison equation with KC-dependent added mass and damping coefficient according to Eq. (1). $F_{I\omega}$ represents the inertia force as predicted by potential flow theory ($C_{a0} = 1.51$). Right: Force harmonic amplitudes for the difference force ΔF.

The next question is whether the incident flow angle matters. Since the experimental set-up was not very well suited for different inflow angles, we performed CFD simulations. Selected results are presented in Figure 5, in terms of crossflow and inline 2ω and 4ω difference force components at $\mathrm{KC} = 16$, for both Cases 1 and 2. We extract three main observations from the figure. The first is that the difference forces are highly sensitive to the inflow angle. The fact that the forces depend on the inflow angle might not be so surprising, given that flow separation is a main effect. However, the sensitivity to angle is perhaps stronger than expected, and clearly indicates that it is not sufficient to study 90° inflow angle only. The second observation is that the 4ω component is also large in general, for other inflow angles than 90°; the amplitude being in general about half that of the 2ω component. The third observation is that the crossflow force is in general considerably larger than the inline force. The magnitude is strikingly large; for the 2ω component it is as large as that of F_ω on each cylinder.

The black diamond markers represent our experimental data. The few experimental data in the figure are not in good quantitative agreement with the numerical simulations, although they are so qualitatively. One reason may be due to that the numerical results were not well converged. A more extensive numerical convergence study is needed, although we do not expect that our main conclusions will change. Another reason can be the high sensitivity to inflow angle. It is of interest to carry out a systematic experimental study with several inflow angles to reveal whether similar trends are present experimentally. Correlation length of the separated flow along the cylinders may also be a candidate for the discrepancy; the cylinder length-to-width ratio is rather large, $L/D = 19$. Preliminary results from three-dimensional type experiments with finite-length cylinders ($L/D = 1, 2$ and 3 where $D = 0.05$m), yields similar magnitudes of the 2ω and 4ω inline and crossflow components as our 2D numerical results do.

A rational hydrodynamic load model is needed for design of such structures. The mean and 2ω load components can be explained qualitatively in the following manner. We apply a simple time-varying incident flow to the drag load in the Morison equation. The velocity magnitude is reduced by a factor during the half cycle where it is downstream of the other cylinder to represent the fact that the rear cylinder experiences a reduced inflow during this half cycle. This provides both a mean and a 2ω load component. However, it does not provide any higher harmonic components.

Neither does it predict the incident flow-angle dependency. In addition to inflow angle and KC-number, the loads will depend on the draft-to-diameter ratio, cross-sectional shape, the configuration which may involve more than two close cylinders and the Reynolds number in the case of blunt pontoon shapes. Combined current and waves will matter. It might be that we will need to use a purely empirical method. Dedicated experiments and CFD for a given design would then be needed. Machine learning may add value.

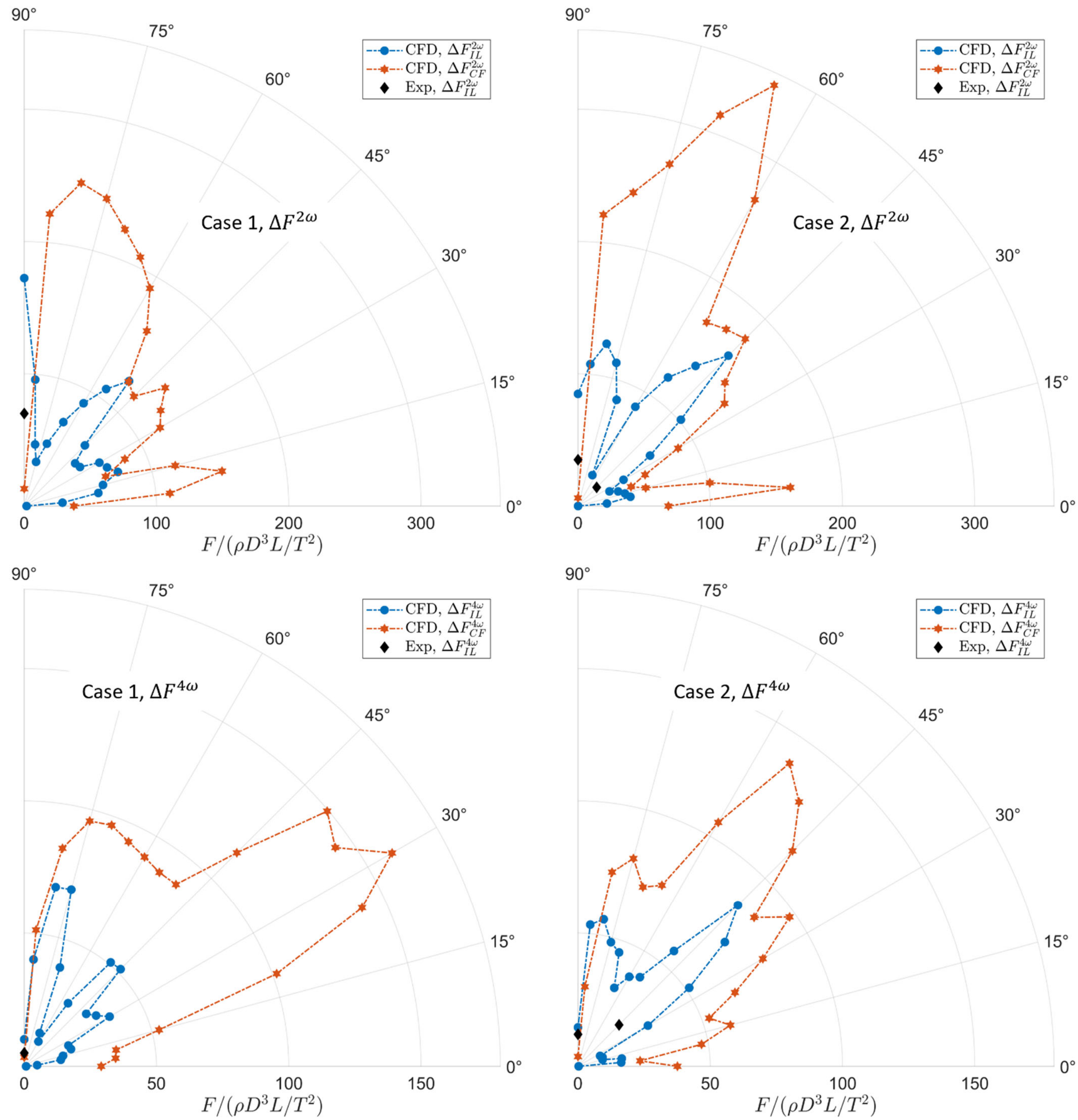

Figure 5. Polar plots of the 2ω and 4ω components of the crossflow (CF) and inline (IL) forces at $\mathrm{KC} = 16$, for Case 1 and Case 2. Most results are by CFD. Our experimental data are represented by the black diamond markers.

Acknowledgements

This work was partly supported by the Research Council of Norway through SFI BLUES, grant number 309281.

References

[1] Zdravkovich, M. M., *Review of Flow Interference Between Two Circular Cylinders in Various Arrangements*, J. Fluids Eng., 1977, 99

[2] Havel, B., Hangan, H. and R. Martinuzzi, *Buffeting for 2D and 3D sharp-edged bluff bodies*, J. Wind Energy and Ind. Aerodyn., 2001, 89

[3] Mentzoni, F., *Hydrodynamic Loads on Complex Structures in the Wave Zone*, PhD thesis NTNU, 2020